Search for pair production of Higgs bosons in the $b\bar{b}b\bar{b}$ final state using proton–proton collisions at $\sqrt{s} = 13$ TeV with the ATLAS detector

A DISSERTATION PRESENTED
BY
BAOJIA TONG
TO
THE DEPARTMENT OF PHYSICS

IN PARTIAL FULFILLMENT OF THE REQUIREMENTS
FOR THE DEGREE OF
DOCTOR OF PHILOSOPHY
IN THE SUBJECT OF
PHYSICS

HARVARD UNIVERSITY
CAMBRIDGE, MASSACHUSETTS
MAY 2018

Thesis advisor: Professor Melissa Franklin Baojia Tong

Search for pair production of Higgs bosons in the $b\bar{b}b\bar{b}$ final state using proton–proton collisions at $\sqrt{s} = 13$ TeV with the ATLAS detector

Abstract

We present a search for Higgs boson pair production, with the $b\bar{b}b\bar{b}$ final state. This analysis uses the full 2015 and 2016 data collected collected by the ATLAS Collaboration at $\sqrt{s} = 13$ TeV, corresponding to $3.2 \pm 0.2\,\text{fb}^{-1}$ of 2015 and $32.9 \pm 1.1\,\text{fb}^{-1}$ of 2016 pp collision data. Improvements with respect to the previous analysis are mainly in the boosted regime, where the resonance signal is between 2500 GeVand 3000 GeV. The data is found to be compatible with the Standard model, and no signs of new physics have been observed. The results are interpreted in the context of the bulk Randall-Sundrum warped extra dimension model with a Kaluza-Klein graviton decaying to hh, with the coupling $k/\bar{M}_{\text{Pl}}$, chosen to be in the allowed range $1.0 - 2.0$. The results are also interpreted with the Type 2 two-Higgs doublet model (2HDM) where the neutral heavy CP-even H scalar decays to hh.

Contents

Listing of figures

Listing of tables

Everything is meaningless.
Even the sentence above.

Acknowledgments

Thanks to everyone the ATLAS collaboration, who has supported this remarkable program and has contributed to every bit of the result in my thesis. Sir Issac Newton said he was standing on the gaint's showlders to see far and deep into the nature. Similarly. I am standing on the ATLAS(member)'s showlders–it's eight stories high so I hope ATLAS doesn't shrug. Without the excellent work on detector design, commisioning, operational works, reconstruction, data processing, performance studies and recommendations, software support, computing support, and analysis discussions and guidance, I could not have completed this thesis. I truely and sincerely thank all ATLAS members for their contributions.

0

Introduction

Why do we look for $hh \to 4b$?

There are two types of analysis in particle physics. The first one is measurement, which yeilds a observable with an uncertainty. This could either imrpove our current knowledge, or show some inconsistency. The other type is search, which generally assumes some new physics model and try to justfy in data wether the new model is justified in some observables. A successful search turns the subject into a measurement, yet a null search result will set a new limit for a given physics model.

After Run 1 of the LHC, with the existence of the Higgs now firmly established, the focus shifted to searches for physics beyond the Standard Model. In particular, searches for high mass resonances

benefit from the LHC's increase to $\sqrt{s} = 13$ TeV in Run 2. The cross section for a generic gluon-initiated resonance with a mass of 2 TeV increases tenfold in Run 2, making searches for high mass resonances a high priority. The newly discovered Higgs can be used as a tool in these searches. After the discovery, the Higgs boson provides a large swath of unmeasured phase space where new physics could be discovered. Higgs pair production in the Standard Model has a low cross section that requires large datasets (on the order of the LHC's lifetime) for full measurement. However, new physics can modify this cross section, especially through new resonances which decay to two Higgs bosons. Such high mass resonances also produce difficult to recognize final state topologies due to the merging of decay products from high momentum Higgs bosons. A search for Higgs pair production in the $HH \rightarrow b\bar{b}b\bar{b}$ final state was performed with 3.2fb^{-1} collected with ATLAS at $\sqrt{s} = 13$ TeV in 2015. The results are presented in this dissertation with a focus on a dedicated signal region for boosted final states. This signal region uses new techniques for recognizing jet substructure and b-tagging to the improve signal acceptance of high mass resonances.

The discovery of the Standard Model (SM) Higgs boson (h)[??] at the Large Hadron Collider (LHC) motivates searches for new physics using the Higgs boson as a probe. In particular, many models predict cross sections for Higgs boson pair production that are significantly greater than the SM prediction. Resonant Higgs boson pair production is predicted by models such as the bulk Randall–Sundrum model[??], which features spin-2 Kaluza–Klein gravitons, G^*_{KK}, that subsequently decay to a pair of Higgs bosons. Extensions of the Higgs sector, such as two-Higgs-doublet models[??], propose the existence of a heavy spin-0 scalar that can decay into $h$pairs. Enhanced non-resonant Higgs boson pair production is predicted by other models, for example those featuring light coloured scalars[?] or direct $t\bar{t}hh$ vertices[??].

Previous searches for Higgs boson pair production have all yielded null results. In the $b\bar{b}b\bar{b}$channel, ATLAS searched for both non-resonant and resonant production in the mass range of 400–3000 GeV using 3.2 fb^{-1} of 13 TeV data[?] collected during 2015. CMS searched for the production of resonances

with masses of 750–3000 GeV[7] using 13 TeV data and with masses 270–1100 GeV with 8 TeV data[8]. Using 8 TeV data, ATLAS has examined the $b\bar{b}b\bar{b}$[9], $b\bar{b}\gamma\gamma$[10], $b\bar{b}\tau^+\tau^-$and $W^+W^-\gamma\gamma$channels, all of which were combined in Ref.[11]. CMS has performed searches using 13 TeV data for the $b\bar{b}\tau^+\tau^-$[12] and $bb\ell\nu\ell\nu$[13] final states, and used 8 TeV data to search for $b\bar{b}\gamma\gamma$[14] in addition to a search in multilepton and multilepton+photons final states[15].

The analyses presented in this paper exploit the dominant $h \to b\bar{b}$decay mode to search for Higgs boson pair production in both resonant and non-resonant production. Two analyses are presented, which are complementary in their acceptance, each employing a unique technique to reconstruct the Higgs boson. The "resolved" analysis is used for hhsystems in which the Higgs bosons have Lorentz boosts low enough that four b-jets can be reconstructed. The "boosted" analysis is used for those hhsystems in which the Higgs bosons have higher Lorentz boosts, which prevents the Higgs boson decay products from being resolved in the detector as separate b-jets. Instead, each Higgs boson candidate consists of a single large-radius jet, and b-decays are identified using smaller-radius jets built from charged-particle tracks.

Both analyses were re-optimized with respect to the former ATLAS publication[7]; an improved algorithm to pair b-jets to Higgs boson candidates is used in the resolved analysis, and in the boosted analysis an additional signal-enriched sample is utilized. The dataset comprises the 2015 and 2016 data, corresponding to 27.5 fb^{-1} for the resolved analysis and 36.1 fb^{-1} for the boosted analysis, with the difference due to the trigger selections used. The results are obtained using the resolved analysis for a resonance mass between 260 and 1400 GeV, and the boosted analysis between 800 GeV and 3000 GeV. The main background is multijet production, which is estimated from data; the subleading background is $t\bar{t}$, which is estimated using both data and simulations. The two analyses employ orthogonal selections, and a statistical combination is performed in the mass range where they overlap. The final discriminants are the four-jet and dijet mass distributions in the resolved and boosted analyses, respectively. Searches are performed for the following benchmark signals: a spin-2

graviton decaying into Higgs bosons, a scalar resonance decaying into a Higgs boson pair, and SM non-resonant Higgs boson pair production.

This dissertation begins by discussing the status of di-Higgs. Chapter 1 gives an overview of double Higgs production in the Standard Model and beyond. Chapter 2 and 3 present details regarding the Large Hadron Collider and the ATLAS experiment. Chapter 4 provides an overview of object reconstruction in ATLAS, with a focus on Muon Segment Seeding. A brief interlude in Chapter 5 on the ATLAS Muon Data Quality, as this has been a focus of my graduate work.

The rest of the dissertation presents a search for Higgs pair production in the $HH \to b\bar{b}b\bar{b}$ channel. Chapter 6 presents an overview of physics object selection, where the Higgs pairs are the result of the decay of a heavy resonance. Chapter 7 discusses the background estimation techinics in detail, followed by Chapter 8, Systematics. Chapter 9 presents the results, and Chapter 10 shows the limits between the boosted regime and the resolved regime, which is sensitive to lower mass resonances and non-resonant Higgs pair production. Finally, the work is summaried a conclusion and brief outlook of future Higgs physics with ATLAS.

Knowledge knows no bounds.

Creator

1

Motivation and Theory

1.1 The Standard Model and the Higgs Boson

The Standard Model(SM) is the best description of the microscopic world [2,3,1,4]. The SM consists of three generations of leptons (e, μ, τ, ν_e, ν , ν_{tau}) and quarks (u, d, c, s, t, b). They all interact via the weak force. In addition, the charged leptons and quarks interact through the EM force and the quarks also interact through the strong force. The SM also has the force mediators. EM force mediates through the photon γ, the strong force meidates through the gluon g, and the weak force mediates through $W^{\pm}$ and Z bosons. The SM predicts everything except the particle's mass, shown in Figure 1.1, which are measured experimentally.

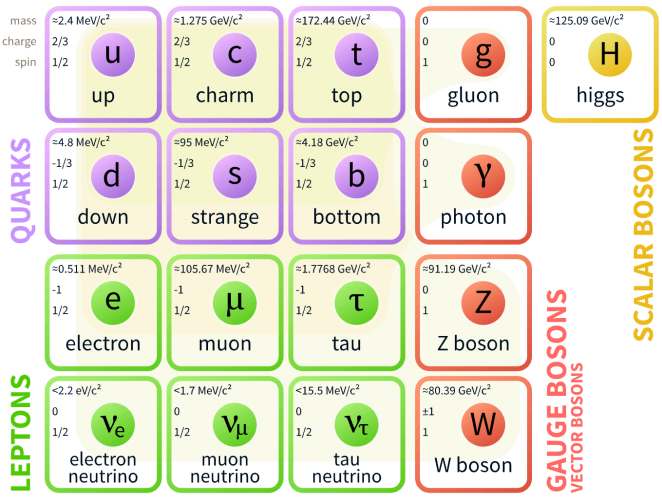

Figure 1.1: Fermions and bosons of the Standard Model and their properties [1].

However, in SM, due to the gauge invriance under $SU(2)_L$, fermions have to be massless in order to have pure left handed states. The bosons must also be massless as required by the gauge principle. The Higgs mechanism introduces a scalr Higgs field with nonzero vaccum expectation values, which impledes and interacts with the propagation of gague bosons and fermions, hence gives them valid mass terms [3]. This broken symmetry of the Standard Model predicts the extra particle degree of freedom as the Higgs boson. The terms inside the Higgs potential are shown in equation 1.1.

Include a shape.

$$V(\varphi_h) = \lambda v^2 \varphi_h^2 + \lambda v \varphi_h^3 + \frac{1}{4}\lambda \varphi_h^4 \tag{1.1}$$

where v corresponds to the vaccum expectation value of the field, determined to be around 246 GeV. The first term gives the Higgs mass, m_h, as $\sqrt{2\lambda}v$, measured to be 125.09 $\pm$ 0.24 GeV. The second term provives an hhh vertex, which corresponds to the trilinear coupling of the Higgs boson. This coupling is also called the Higgs self-coupling. This means that a two Higgs production, known as di-Higgs or Higgs pair production, can happen through a single Higgs even within the Standard Model. Therefore, Higgs pair production is extremely interesting to study because it is the only

direct measurement of the λ parameter of the Higgs potential.

1.2 Standard Model di-Higgs at the LHC

Through the Higgs self-coupling, di-Higgs events could be created at the LHC. One single Higgs produced with enough energy could split into two on-shell Higgs. Another way to produce di-Higgs is through a rectangular top/bottom quark loop. These are the two main processes that contribute most to the production at the LHC. Other Feynman diagrams exist but will have higher order loops and thus smaller cross section.

Interestingly, according to the SM, the two diagrams have opposite signs and destructively interfere, and hence the production cross section for di-Higgs as a function of the strengh of Higgs-self coupling is a non trivial distribution.

Gluon fusion remains by far the dominant production mode. The total cross section at the NNLO with current calculations is 34 $fb^{-1}$for p-p collisions at 13 TeV.

There is much literature about modifications of Higgs self coupling. Using the SM measurements and their precisions, the self coupling parameter could be constrained to an order of magnitude, see note.

1.3 Beyond the Standard Model Physics di-Higgs at the LHC

BSM physics could significantly enhance the production of di-Higgs at the LHC. This is separated into two categories: non-resonant and resonant productions. The non-resonant production generally refers to modifications of the Higgs couplings, either the Higgs self-coupling or the Higgs-top couplings. Resonant production refers to a particle with invariant mass greater than twice the

Higgs mass decays directly into two Higgs bosons. The difference also comes from the distribution of the di-Higgs invariant mass at the truth level: in the non-resonant case typically has no clear peak, whereas in the resonant case the invariant mass distribution forms a peak with model-depdent width.

With the increased center of mass collison energy, the production cross section grows, particularly for heavy particles above TeV.

1.4 Di-Higgs Decay and LHC search perspectives

Di-Higgs decay is the combination of single Higgs decays. The partile width for Higgs to fermions and bosons (one of them is off-shell) at tree level are shown in equation 1.2[5]:

$$\Gamma(h \to \bar{f}f) = \frac{N_c\sqrt{2}G_F m_f^2 m_h}{8}$$
$$\Gamma(h \to VV^*) = \frac{1}{2}\int_0^{M_H^2} \frac{dq_1^2 M_V\Gamma_V}{(q_1^2-M_V^2)^2+M_V^2\Gamma_V^2}\int_0^{(M_H-q_1)^2} \frac{dq_2^2 M_V\Gamma_V}{(q_2^2-M_V^2)^2+M_V^2\Gamma_V^2}\frac{\sqrt{2}}{32}\frac{v G_F m_h^3}{}\sqrt{\lambda(q_1^2,q_2^2;m_h^2)}[\lambda(q_1^2,q_2^2;m_h^2)+12\frac{q_1^2q_2^2}{m_h^2}] \tag{1.2}$$

where N_c is the number os colors, m_f is the fermion mass, G_F is the Fermi constant. Hence, given the measured Higgs mass, tthe larges brancing ratio is to the $b\bar{b}$. Although there is no direct coupling between h and $\gamma\gamma$ at tree level, this decay can happen through W or top loops.

A man who procrastinates in his choosing will inevitably
have his choice made for him by circumstance.

Hunter S. Thompson

2

The Large Hadron Collider

The Large Hadron Collider (LHC) is a proton-proton collider at the European Organization for Nuclear Research (CERN) laboratory in Geneva, Switzerland[6]. In order to reach the physics goals, the two most important design parameters for a collider are beam energy and luminosity. This chapter will cover how these two parameters are reached by the LHC, and the final design and layout.

2.1 Beam Energy

In order to probe the quarks and gluons inside, protons need to be accelerated to high energies. For a charged particle, charge Z (for protons, $Z = 1$) and momentum p, its trajectory within a mag-

netic field $B(s)$ is described by the deflection angle $d\vartheta$, with radius ϱ.

$$d\vartheta = \frac{ds}{\varrho} = \frac{ZB(s)ds}{p} \tag{2.1}$$

Integrate this angle over the circumference:

$$\oint_C d\vartheta = 2\pi = \frac{1}{p}\oint_C B(s)ds \tag{2.2}$$

Thus the momentum ($\sim$ energy) of the charged particle is:

$$p = \frac{1}{2\pi}\oint_C B(s)ds = 1 \times 47.7[\frac{MeV}{cTm}]\oint_C B(s)ds \tag{2.3}$$

In order to achieve a designed center of mass energy of $\sqrt{s} = 14$ TeV, the momentum of the proton is 7 TeV. Given the technology constrains, the Niobium Titanium magnetic dipole is 14.3 meters in length, and while cooled by superfluid helium to a temperature of 1.9 Kelvin, can generate 8.33 Tesla magnetic field. Therefore, according to Eq2.3, the LHC needs 1232 such magnets for steering. Additionally, 6800 superconducting magnets are used to focus the beam, squeeze the beam, correct the trajectory, and damp oscillation in beam position.

2.2 Luminosity

In order to study certain physics events, the production rate affects the experiment. The rate of a specified physics process $R_{\text{phy}} = L\sigma$, where L is the instantaneous luminosity ($m^{-2}s^{-1}$) the collider, and $\sigma(m^2)$ the physics process' cross section. The instantaneous luminosity is could be controlled and affects the experiment data taking length. For a Gaussian beam profile, It is defined in Eq2.4 [7]:

$$L = \frac{N_b^2 n_b f_{\text{rev}}\gamma_r}{4\pi\varepsilon_n\beta^*}F \tag{2.4}$$

In the above Eq2.4:

- N_b is the number of protons per bunch;
- n_b is the number of bunches per beam; n_b cannot be too large due to potential beam loss damages on the accelerator and detector;
- f_{rev} is the proton revolution frequency; or the ratio of the circumference of LHC, 26.7 km, and the speed of light.
- γ_r is the relativistic Lorentz factor for the protons;
- ε_n is the average beam spread in the transverse plane;
- β^* is a measure of the beam spread in the longitudinal direction; affected by focusing magnets;
- F is a reduction factor for the angle beams are colliding; smaller crossing angles could cause larger spread in the longitudinal direction.

The instantaneous luminosity can also be written as the ratio of the rate of inelastic collisions to the inelastic cross section σ_{inel} [10].

$$L = \frac{R_{\text{inel}}}{\sigma_{\text{inel}}} = \frac{\mu n_b f_{\text{rev}}}{\sigma_{\text{inel}}} \tag{2.5}$$

where, μ is the number of interactions per bunch crossing. At each bunch crossing, multiple proton-proton collide, and the collisions without the highest center of mass energy are called "pileup" interactions. The averaged collision activities over all bunch crossings, $\langle\mu\rangle$, is a measurement of the level of pileup in the detector. For High Luminosity LHC, the expected $\langle\mu\rangle$ is 200. The higher number of pileup, the higher total collision events are produced, but is harder for the detectors to distinguish each collision separately.

Parameter [unit]	Nominal design value	2015 Operating value	2016 Operating value
Beam Energy [TeV]	7	6.5	6.5
Peak L [$cm^2\ s^{-1}$]	10^{34}	5×10^{33}	1.25×10^{34}
Bunch spacing [ns]	25	25	25
n_b [10^{11} p/bunch]	1.15	1.15	1.12
N_b [bunch]	2808	1825	2220
f_{rev} [kHz]	11245	11245	11245
ε_n [mm mrad]	3.5	3.5	2
β^* [cm]	55	80-40	40
F	0.84	0.84	0.59
$\langle\mu\rangle$	19	13	41

Table 2.1: LHC nominal [6] and operational parameters in 2015 [8] and 2016 [9].

The target peak instantaneous luminosity for both the ATLAS and CMS experiments is $L = 10^{34}\ cm^{-2}s^{-1}$ [6], which is already exceeded in 2016. The main parameters of the LHC beam and performance are shown in Table 2.1. At the nominal LHC conditions, the beam energy is about 360 MJ.

2.3 Layout

Protons accelerated in the LHC originate from a red bottle of hydrogen gas. The whole series take around 4 + 20 (LHC only) minutes:

- An electric field strips the electrons from the hydrogen to create protons;
- A linear particle accelerator, Linac 2, accelerates the protons to 50 MeV;
- The Proton Synchrotron Booster (PSB) accelerates the protons to 1.4 GeV;
- The Proton Synchrotron (PS) accelerates the protons to 25 GeV;
- The Super Proton Synchrotron (SPS) accelerates the protons to 450 GeV; it sends the protons in bunch trains;
- The LHC accelerates the protons in a series of Radio Frequency cavities to the final TeV energies.

Interaction points (IP) are where the two proton beams focused and collided. Only a part of the protons in the bunch collide, and the rest remains in LHC and travels to the next interaction point.

ATLAS (A Toroidal LHC ApparatuS), CMS (the Compact Muon Solenoid), ALICE (A Large Ion Collider Experiment), and LHCb[11,12,13,14] are the four main experiments. They are located at the IPs of the accelerator. Figure 2.1 shows a schematic of the LHC ring and its experiments.

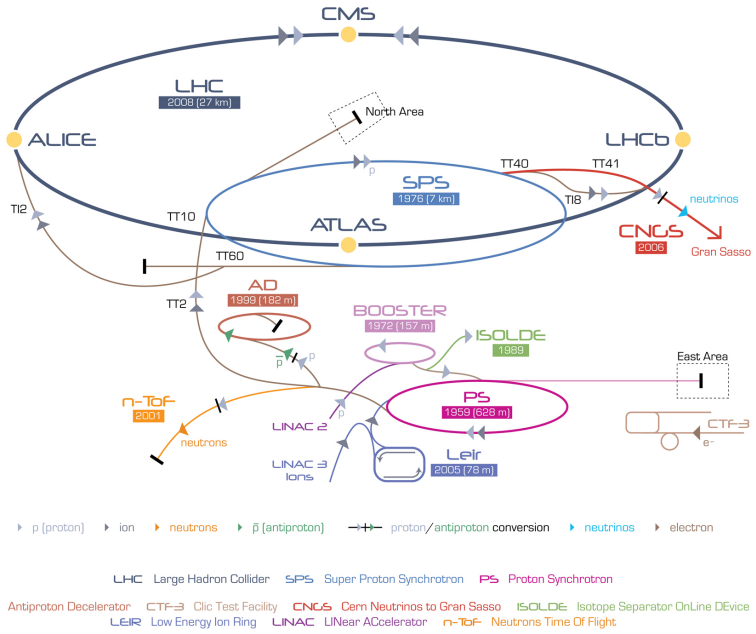

Figure 2.1: A schematic view of the LHC ring[7]. LINAC2, Booster, PS, SPS, and LHC accelerate the protons in order. Four main experiments are located at interaction points along the ring. ATLAS and CMS are general purpose experiments, while ALICE focuses on heavy ion collisions and LHCb is dedicated to B physics.

Ugliness is in a way superior to beauty because it lasts.

Serge Gainsbourg

3

Detector

The ATLAS experiment[15] at the LHC is a multipurpose particle detector with a forward-backward symmetric cylindrical geometry and a near 4π coverage insolid angle. ATLAS uses a right-handed coordinate system with its origin at the nominal interaction point (IP) in the centre of the detector and the z-axis along the beam pipe. The x-axis points from the IP to the centre of the LHC ring, and the y-axis points towards the sky. Cylindrical coordinates (r, ϕ) are used in the transverse plane, ϕ being the azimuthal angle around the z-axis. The pseudorapidity is defined in terms of the polar angle ϑ as $\eta = -\ln\tan(\vartheta/2)$. Angular distance is measured in units of $\Delta R \equiv \sqrt{(\Delta\eta)^2 + (\Delta\phi)^2}$. The ATLAS detector consists of an inner tracking detector (ID) surrounded by a thin superconducting solenoid providing a 2T axial magnetic field, electromagnetic (EM) and hadronic calorimeters, and a muon spectrometer (MS).

3.1 Inner Detector

The ID covers the pseudorapidity range $|\eta| < 2.5$. It has three parts: silicon pixel, silicon microstrip, and straw-tube transition-radiation tracking detectors. An additional pixel detector layer[16], inserted at a mean radius of 3.3 cm, is used in the Run-2 data-taking and improves the identification of b-jets[17].

Material of ATLAS Inner Detector for Run 2 of the LHC. note.

3.2 Calorimeter

Lead/liquid-argon (LAr) sampling calorimeters provide EM energy measurements. A steel/scintillator-tile hadronic calorimeter covers the central pseudorapidity range ($|\eta| < 1.7$). The endcap and forward regions are instrumented with LAr calorimeters for both the EM and hadronic energy measurements up to $|\eta| = 4.9$.

3.3 MuonSpectrometer

The muon spectrometer surrounds the calorimeters and includes three large superconducting air-core toroids. The field integral of the toroids ranges between 2 and 6 T/m for most of the detector. The MS includes a system of precision tracking chambers and triggering chambers.

3.4 Trigger and Data Aquasition

A dedicated trigger system is used to select events[18]. The first-level trigger is implemented in hardware and uses the calorimeter and muon detectors to reduce the accepted event rate to 100 kHZ. This is followed by a software-based high-level trigger that reduces the accepted event rate to 1 kHZ on average.

To avoid too high accept rates for certain triggers, the triggers are often prescaled, which means the accepted events get rejected at the prescale. For example, a prescale of two means only every second event passing all trigger conditions gets accepted.

For further trigger information, see 2015 note and 2016 updates.

4

Conclusion

Di-Higgs search has a short history, but will have a long future. This thesis presents a search for both resonant and non-resonant production of pairs of Standard Model Higgs bosons has been carried out in the dominant $b\bar{b}b\bar{b}$ channel, using 27.5–36.1 fb^{-1} of LHC pp collision data at $\sqrt{s} =$ 13 TeV collected by ATLAS in 2015 and 2016. The search sensitivity of this analysis exceeds that of the previous analysis of the $\sqrt{s} = 13$ TeV 2015 dataset[3] for non-resonant signal and also across the entire mass range of 260-3000 GeV for the resonance search, with significantly improvement in the high mass resonance sensitivities. The resolved analysis has each $h \to b\bar{b}$ reconstructed as two separate b-tagged jets, and the boosted analysis has each $h \to b\bar{b}$ reconstructed as a single large-radius jet associated with at least one small-radius b-tagged track-jet. The estimated background consists mainly of multi-jet and $t\bar{t}$ events.

No significant excess is observed in the data. The largest deviation from the background-only hypothesis is observed for narrow signal models at a mass of 280 GeV in the resolved analysis, with a global significance of 2.3σ. This excess could be a trigger-turn on combined with kinematic selection effect and might not last with more data. Upper limits on the production cross section times branching ratio to the $b\bar{b}b\bar{b}$ final state are set for a narrow-width scalar and for spin-2 resonances. The 95% CL upper limit on the non-resonant production is 147 fb, which corresponds to 13.0 times the SM expectation.

Future improvement with the rest of $\sqrt{s} = 13$ TeV Run II could come from improving b-tagging, especially in the high p_{T}region. Advanced trigger technologies and selections will increase the data rate, and better jet energy and mass resolution will increase the purity in selection. With the larger dataset and improvements in physics performance, it is possible to reach twice as the current sensitivity of resonance searches. For non-resonance searches, an order of 10 times the SM expectation is more sensible at the end of Run II.

For longer term perspectives, di-Higgs measurements will continue to be one of the most important analysis that help constraining our understanding of physics beyond the Standard Model. Given the current status, it is possible that in fifteen to twenty years there will be no new discovery, and the experiments at the LHC will be able to constrain the Higgs self-coupling within unity.

As humans, we have a limited life. However, physics, as well as the understanding of the universe, is an endless journey. I sincerely hope that my biased prediction of the future of Higgs physics will be wrong, but nevertheless I am deeply honored to be a small part of this odyssey towards Veritas.

References

[1] C. Patrignani et al. Review of Particle Physics. *Chin. Phys.*, C40(10):100001, 2016. doi: 10.1088/1674-1137/40/10/100001.

[2] David Griffiths. *Introduction to elementary particles*. 2008.

[3] Christopher G. Tully. *Elementary particle physics in a nutshell*. 2011.

[4] Matthew D. Schwartz. *Quantum Field Theory and the Standard Model*. Cambridge University Press, 2014. ISBN 1107034736, 9781107034730.

[5] Abdelhak Djouadi. Decays of the Higgs bosons. In *Quantum effects in the minimal supersymmetric standard model. Proceedings, International Workshop, MSSM, Barcelona, Spain, September 9-13, 1997*, pages 197–222, 1997.

[6] Lyndon R Evans and Philip Bryant. LHC Machine. *J. Instrum.*, 3:S08001. 164 p, 2008. URL https://cds.cern.ch/record/1129806. This report is an abridged version of the LHC Design Report (CERN-2004-003).

[7] Lyndon Evans. The Large Hadron Collider. *Annual Review of Nuclear and Particle Science*, 61(1):435–466, 2011. doi: 10.1146/annurev-nucl-102010-130438.

[8] Paul Collier for the LHC team. LHC Machine Status. CERN Resource Review Board, 2015. URL https://cds.cern.ch/record/2063924/files/CERN-RRB-2015-119.PDF.

[9] Giulia Papotti for the LHC team. LHC Machine Status Report. CERN Resource Review Board, 2016. URL https://indico.cern.ch/event/563488/contributions/2277292/attachments/1340292/2019570/20160921_LHCC.pdf.

[10] ATLAS Collaboration. Luminosity Determination in pp Collisions at $\sqrt{s} = 7$ TeV Using the ATLAS Detector at the LHC. *Eur. Phys. J.*, C 71:1630, 2011. doi: 10.1140/epjc/s10052-011-1630-5.

[11] ATLAS Collaboration. The ATLAS experiment at the CERN Large Hadron Collider. *JINST*, 3:S08003, 2008. doi: 10.1088/1748-0221/3/08/S08003.

[12] CMS Collaboration. The CMS experiment at the CERN LHC. *Journal of Instrumentation*, 3 (08):S08004, 2008. URL http://stacks.iop.org/1748-0221/3/i=08/a=S08004.

[13] LHCb Collaoration. The LHCb Detector at the LHC. *JINST*, 3:S08005, 2008. doi: 10.1088/1748-0221/3/08/S08005.

[14] ALICE Collaboration. The ALICE experiment at the CERN LHC. *Journal of Instrumentation*, 3(08):S08002, 2008. URL http://stacks.iop.org/1748-0221/3/i=08/a=S08002.

[15] ATLAS Collaboration. The ATLAS Experiment at the CERN Large Hadron Collider. *JINST*, 3:S08003, 2008. doi: 10.1088/1748-0221/3/08/S08003.

[16] ATLAS Collaboration. ATLAS Insertable B-Layer Technical Design Report. CERN-LHCC-2010-013. ATLAS-TDR-19, Sep 2010. URL https://cds.cern.ch/record/1291633.

[17] ATLAS Collaboration. Expected performance of the ATLAS *b*-tagging algorithms in Run-2. ATL-PHYS-PUB-2015-022, 2015. URL https://cds.cern.ch/record/2037697.

[18] ATLAS Collaboration. Performance of the ATLAS Trigger System in 2015. *Eur. Phys. J. C*, 77:317, 2017. doi: 10.1140/epjc/s10052-017-4852-3.